

Infrared Gluon and Ghost Propagators from Lattice QCD

Results from large asymmetric lattices

O. Oliveira and P. J. Silva

Centro de Física Computacional, Universidade de Coimbra, 3004 516 Coimbra, Portugal

Received: date / Revised version: date

Abstract. We report on the infrared limit of the quenched lattice Landau gauge gluon and ghost propagators as well as the strong coupling constant computed from large asymmetric lattices. The infrared lattice propagators are compared with the pure power law solutions from Dyson-Schwinger equations (DSE). For the gluon propagator, the lattice data is compatible with the DSE solution. The preferred measured gluon exponent being ~ 0.52 , favouring a null zero momentum propagator. The lattice ghost propagator shows finite volume effects and, for the volumes considered, the propagator does not follow a pure power law. Furthermore, the strong coupling constant is computed and its infrared behaviour investigated.

PACS. 12.38.-t Quantum chromodynamics – 11.15.Ha Lattice gauge theory – 12.38.Gc Lattice QCD calculations – 12.38.Aw General properties of QCD – 14.70.Dj Gluons – 14.80.-j Other particles

1 Introduction

In the pure gauge SU(3) Yang-Mills theory, a number of authors has been using first principles approaches, i.e. Dyson-Schwinger equations (DSE) and lattice QCD methods, to investigate the infrared gluon and ghost propagators in Landau gauge, respectively,

$$D_{\mu\nu}^{ab}(k) = \delta^{ab} \left(\delta_{\mu\nu} - \frac{k_\mu k_\nu}{k^2} \right) D(k^2), \quad (1)$$

$$G_{\mu\nu}^{ab}(k) = -\delta^{ab} G(k^2), \quad (2)$$

and the strong coupling constant [1] defined as

$$\alpha_S(k^2) = \alpha_S(\mu^2) Z_{ghost}^2(k^2) Z_{gluon}(k^2); \quad (3)$$

$Z_{ghost}(k^2) = k^2 G(k^2)$ and $Z_{gluon}(k^2) = k^2 D(k^2)$ are the ghost and gluon dressing functions. In part, these studies have been triggered by the solution of the DSE [2] which assuming infrared ghost dominance and infrared finiteness of the loop-integrals predicts pure power laws for the dressing functions

$$Z_{gluon}(k^2) = A (k^2)^{\kappa'}, Z_{ghost}(k^2) = B (k^2)^{-\kappa}. \quad (4)$$

Moreover, the DSE solution relates the exponents of the two propagators, $\kappa' = 2\kappa$, and predicts a finite strong coupling constant at zero momentum. The infrared solution predicts a null gluon propagator and an infinite ghost propagator at zero momentum ($\kappa > 0.5$). The infrared behaviour of the propagators can be related to gluon confinement criteria [3]. Looking at this particular DSE solution

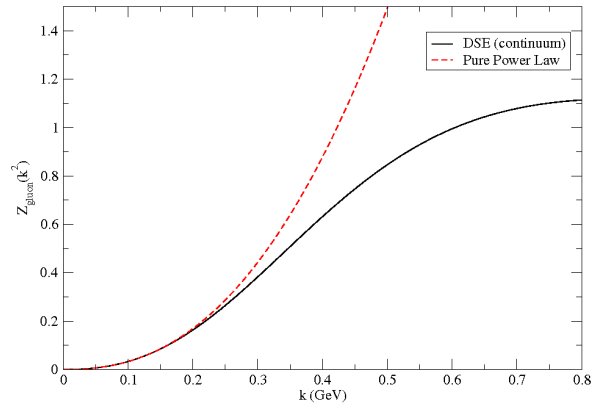


Fig. 1. DSE gluon dressing function versus the pure power law solution. The data is taken from [4].

for the gluon propagator, the comparison with the pure power law, see figure 1, shows that the pure power law is valid only for momenta $k < 200$ MeV.

One should have in mind that the solution discussed above is a particular solution of the DSE. Indeed, there are, in the literature, different types of solutions for the DSE [5]. Moreover, the authors of [6] have investigated a generalization of the conditions assumed in [2] and found alternative behaviours for the infrared gluon and ghost propagators. Given the different scenarios, it would be important if lattice QCD can provide additional input, helping to check if any of the proposed solutions reproduces the lattice data. For a recent discussion on the infrared behaviour of the gluon and ghost propagators see [7].

For the lattice it is a challenge to investigate such low momenta. A possible way out is to consider large asymmetric lattices, which, despite the lattice effects which requires a careful estimation, allows to access the momenta required in such an investigation [8,9,10,11]. Here we report on the gluon, ghost and strong coupling constant computed from large asymmetric lattices.

2 Gluon Propagator

In [11] we have investigated the infrared lattice Landau gauge gluon propagator. For notation and definitions see the above cited article. The simulation uses the Wilson action with $\beta = 6.0$ and combine a number of asymmetric lattices $L^3 \times 256$, $L = 8, 10, 12, 14, 16, 18$ to allow for $L \rightarrow +\infty$ extrapolation. In what concerns the time direction, the $16^3 \times 256$ and $16^3 \times 128$ gluon propagators were compared and no deviations were observed. This suggests that we have a sufficient number of points in the time direction.

For the lattices with the largest time direction, the minimum momenta being accessed is 47 MeV, while for the $16^3 \times 128$ the minimum momenta is 98 MeV. In what concerns the fits to a pure power law, it was observed that the largest lattices ($T = 256$) can reproduce well a pure power law in the infrared. This behaviour was not observed for the lattice $16^3 \times 128$, with the fits to the pure power law having a $\chi^2/d.o.f > 10$. This result is not surprising, given the smallest range of momenta available for this lattice (97 - 294 MeV) and the validity of the pure power law. Nevertheless, the $16^3 \times 128$ will allow us to estimate Gribov copies effects, within reasonable computation efforts.

Let us summarize the results reported in [11] using the simulations with the largest time extension. Asymmetric lattices have clearly lattice size effects (see figures 4 and 5 of [11]). However, the extrapolation towards $L \rightarrow +\infty$ is smooth. The extrapolated gluon propagator was well reproduced by a pure power law, with measured $\kappa = 0.49 - 0.52$. Clearly, the lattice data favors $\kappa \sim 0.52$, in agreement with other theoretical estimates. Unfortunately, presently one cannot provide yet a definitive answer concerning the value of the gluon propagator at zero momentum. We are currently engaged in trying to give such an answer.

For the $16^3 \times 128$ lattice, Gribov copies effects were estimated by comparing the gluon propagator computed from 164 configurations gauge fixed as in [11] (SD in the figures) and the same gauge configurations gauge fixed using the method described in [12] (CEASD in the figures), which aims to estimate the absolute maximum of the gauge fixing function. The gluon propagator given by the two methods is, within the statistical precision of the simulation, the same (see figure 2), with the various fits to the lattice data (infrared, ultraviolet, all momenta) reproducing similar results. Therefore, in what concerns the gluon propagator, no visible effects of Gribov copies are observed.

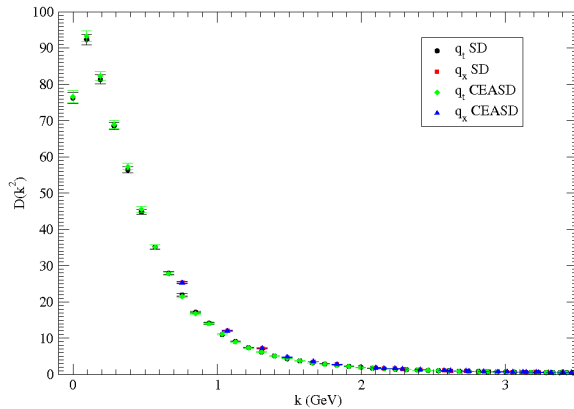


Fig. 2. Bare gluon propagator for $16^3 \times 128$.

3 Ghost Propagator

The ghost propagator [13] was computed using two different methods [14,15]. The first allows, by solving once a linear system, to access all momenta. Its drawback being that, by computing $G(x,0)$, the statistical errors in the propagator are much larger. The second method requires an inversion of the same linear system per momentum, therefore is much more computational demanding. However, for the momenta considered, it provides the propagator with better statistical accuracy. Having the propagator computed with the two methods, allows for a cross-check of the calculation.

In the following, for the ghost propagator the colour average was always performed. For the propagator computed with the [14] method, in order to reduce the statistical error, seven different sources for the linear system were considered and their result averaged.

For the ghost propagator, one observes sizeable finite size effects (see figure 3), in agreement with the SU(2) study [16], and a very sign of clear Gribov copies effects for a large range of momenta.

In what concerns finite volume effects, figure 3 show that the ghost dressing function is enhanced when the lattice volume is increased. Moreover, the largest volumes have a largest dressing function and, for the smallest momenta, the derivatives of the dressing function seem to become smaller when the volume increases.

In what concerns the effects due to Gribov copies, figure 3 shows that the effect cannot be eliminated by the renormalization of the propagator.

To study the compatibility of the ghost propagator with the DSE solutions, the lattice data was fitted to pure power laws and naïve corrections to the pure power law. It came out that the data is not described by any of the functions considered. Given the results of a similar study for the $16^3 \times 128$ gluon propagator, this result is not a complete surprise.

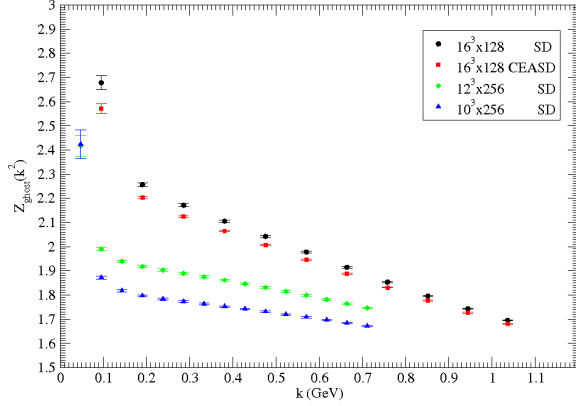


Fig. 3. Bare ghost dressing functions for a $16^3 \times 128$ and $L^3 \times 256$, $L = 10, 12$ lattices.

4 Strong Coupling Constant

The strong coupling constant as defined by equation (3) is reported in figure 4 for the $16^3 \times 128$ lattice and CEASD gauge fixing method. For the other simulations and the SD method, the measured coupling constants are, qualitatively, similar. Figure 5 show the strong coupling constant for small momenta, for all the simulations considered previously.

The simulations show a decreasing lattice strong coupling constant for small momenta, in agreement with previous lattice calculations [17,18]. From our simulation, it is not clear if $\alpha_S(0)$ is null. We have tried a number of fits to the strong coupling constant as a function of the momenta, some requiring $\alpha_S(0) = 0$ and some living $\alpha_S(0)$ as a free parameter, and the data can be equally described by the two situations. For small momenta, only for the $16^3 \times 128$ data and the CEASD gauge fixing algorithm, α_S is described by a pure power law $\alpha_S(q^2) = (q^2)^{\kappa_\alpha}$, with $\kappa_\alpha = 0.69$ suggesting a null zero momentum strong coupling constant. Note, however, that the data shows that α_S increases with the lattice volume (see figure 5). Note, also, the effect of the Gribov copies on the strong coupling constant.

References

1. For a review on strong coupling constant see, for example, G. M. Prosperi, M. Raciti, C. Simolo, hep-ph/0607209.
2. L. von Smekal, A. Hauck, R. Alkofer, Phys. Rev. Lett. **79** (1997) 3591; Ann. Phys. **267** (1998) 1.
3. For a review on DSE gluon and ghost propagators see, for example, C. S. Fischer, J. Phys. **G32** (2006) R253 [hep-ph/0605173].
4. C. S. Fischer, M. R. Pennington, Phys. Rev. **D73** (2006) 034029.
5. A. C. Aguillar A. A. Natale, P. S. Rodrigues da Silva, Phys. Rev. Lett. **90** (2003) 152001; A. C. Aguillar, A. A. Natale, JHEP **0408** (2004) 057.
6. Ph. Boucaud, J. P. Leroy, A. Le Yaouanc, A. Y. Lokhov, J. Micheli, O. Pène, J. Rodríguez-Quintero, C. Roiesnel, hep-ph/0507104.

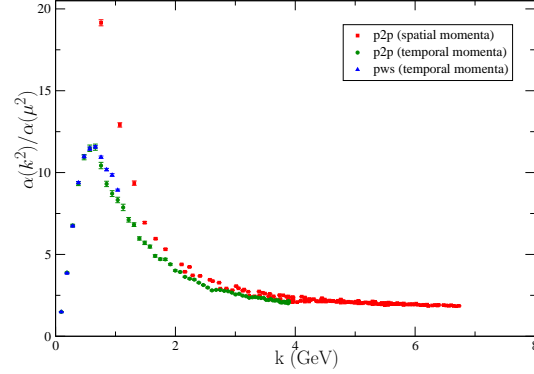


Fig. 4. Strong coupling constant for $16^3 \times 128$ configurations for the CEASD gauge fixing method; “p2p” (“pws”) stands for the ghost computed using [14] ([15]) method.

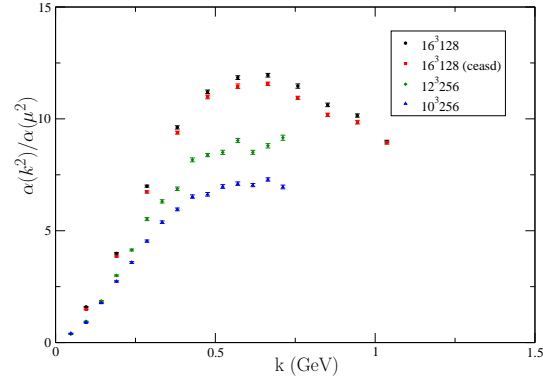


Fig. 5. Small momenta strong coupling for all the simulations.

7. C. S. Fischer, J. M. Pawłowski, hep-th/0609009.
8. O. Oliveira, P. J. Silva, AIP Conf. Proc. **756** (2005) 375.
9. P. J. Silva, O. Oliveira, PoS **LAT2005** (2006) 286.
10. O. Oliveira, P. J. Silva, PoS **LAT2005** (2006) 287.
11. P. J. Silva, O. Oliveira, Phys. Rev. **D74** (2006) 034513 [hep-lat/0511043].
12. O. Oliveira, P. J. Silva, Comput. Phys. Commun. **158** (2004) 73 [hep-lat/0309184].
13. The definitions concerning the ghost propagator can be found in the articles where the lattice ghost propagator has been computed so far.
14. H. Suman, K. Schilling, Phys. Lett. **B373** (1996) 314 [hep-lat/9512003].
15. A. Cucchieri, Nucl. Phys. **B508** (1997) 353 [hep-lat/9705005].
16. A. Cucchieri, T. Mendes, Phys. Rev. **D73** (2006) 071502 [hep-lat/0602012].
17. S. Furui, H. Nakajima, PoS **LAT2005** 291 [hep-lat/0509035]; hep-lat/0609024.
18. A. Sternbeck, E.-M. Ilgenfritz, M. Müller-Preussker, Phys. Rev. **D73** (2006) 014502 [hep-lat/0510109]; Phys. Rev. **D72** (2005) 014507 [hep-lat/0506007].